

20 ABSTRACT

21

22 Small extracellular vesicles (sEVs) released from the extravillous trophoblast (EVT)
23 are known to regulate uterine spiral artery remodeling during early pregnancy. The
24 bioactivity and release of these sEVs differ under differing oxygen tensions and in
25 aberrant pregnancy conditions. Whether the placental cell-derived sEVs released
26 from the hypoxic placenta contribute to the pathophysiology of preeclampsia is not
27 known. We hypothesize that, in response to low oxygen tension, the EVT packages
28 a specific set of proteins in sEVs and that these released sEVs interact with
29 endothelial cells to induce inflammation and increase maternal systemic blood
30 pressure. Using a quantitative MS/MS approach, we identified 507 differentially
31 abundant proteins within sEVs isolated from HTR-8/SVneo cells (a commonly used
32 EVT model) cultured at 1% (hypoxia) compared with 8% (normoxia) oxygen. Among
33 these differentially abundant proteins, 206 were upregulated and 301 were
34 downregulated ($p < 0.05$), and they were mainly implicated in inflammation-related
35 pathways. *In vitro* incubation of hypoxic sEVs with endothelial cells, significantly
36 increased ($p < 0.05$) the release of GM-CSF, IL-6, IL-8, and VEGF, when compared to
37 control (*i.e.*, cells without sEVs) and normoxic sEVs. *In vivo* injection of hypoxic sEVs
38 into pregnant rats significantly increased ($p < 0.05$) mean arterial pressure with
39 increases in systolic and diastolic blood pressures. We propose that oxygen tension
40 regulates the release and bioactivity of sEVs from EVT and that these sEVs regulate
41 inflammation and maternal systemic blood pressure. This novel oxygen-responsive,
42 sEVs signaling pathway, therefore, may contribute to the physiopathology of
43 preeclampsia.
44

45 List of abbreviations

46 Small extracellular vesicles (sEVs); Sequential Window Acquisition of All Theoretical
47 Mass Spectra (SWATH); mass spectrometry (MS/MS); Granulocyte-macrophage
48 colony-stimulating factor (GM-CSF); Interleukin 6 (IL-6); Interleukin 8 (IL-8); Vascular
49 endothelial growth factor (VEGF); extravillous trophoblast (EVT); Preeclampsia (PE);
50 small non-coding RNA (miRNAs); antiphospholipid antibody (aPL);
51 syncytiotrophoblast derived extracellular vesicles (STBEVs); cluster of differentiation
52 63 (CD63); Tumor susceptibility gene 101 (TSG101); Code of Federal Regulation
53 (CFR); National Association of Testing Authorities (NATA); A Short Tandem Repeat
54 (STR); Deoxyribonucleic acid (DNA); Phosphate-buffered saline (PBS); size-
55 exclusion chromatography (SEC); Gene Set Enrichment Analysis (GSEA); Ingenuity
56 Pathway Analysis (IPA); Information-dependent acquisition (IDA); Placental growth
57 factor (PIGF); Soluble fms-like tyrosine kinase-1 (sFLT-1); endothelial nitric oxide
58 synthase (eNOS); nitric oxide (NO); Soluble endoglin (sEng); Glucocorticoids (GC);
59 Human umbilical vein endothelial cell (HUVECs)
60

61

62 **Clinical Perspectives:**

63

64 • Preeclampsia is a common obstetric complication that results in
65 significant maternal and neonatal morbidity and mortality. The
66 underlying pathophysiology of preeclampsia is poorly understood.

67

68 • Low oxygen tension (i.e., hypoxia) predominates in preeclamptic
69 placenta and drives the excessive release of small extracellular
70 vesicles (sEVs), thought to be exosomes, into the maternal circulation,
71 causing vascular endothelial cell dysfunction.

72

73 • This study demonstrated that hypoxia modified the content and
74 bioactivity of sEVs in vitro and in vivo, leading to inflammation and an
75 increase in systemic blood pressure in pregnant rats, mimicking the
76 hypertensive changes seen in preeclampsia.

77

78 • Our finding suggests that the extracellular trophoblast derived sEVs
79 might have a role in the pathophysiology of preeclampsia.

80

81 INTRODUCTION

82 Optimal pregnancy outcome is dependent upon successful fertilization, endometrial
83 implantation, and placentation to support blastocyst development (1). Extravillous
84 trophoblast plays a significant role in establishing fetomaternal circulation via
85 remodeling of the uterine spiral arteries and placentation (2). During early
86 pregnancy (< 10-12 weeks), endovascular extravillous trophoblasts occlude uterine
87 spiral arteries to maintain a low oxygen environment (~2-3% O₂), which is essential
88 for normal embryogenesis and organogenesis (2). Subsequently, extravillous
89 trophoblast replaces the vascular endothelial and smooth muscle cells to remodel
90 the uterine spiral arteries with the formation of high capacitance and low resistance
91 vessels, enabling adequate placental perfusion (3). In addition, extravillous
92 trophoblast invades the uterine glands and veins and connect all these luminal
93 structures to form the inter-villous space (4). When extravillous trophoblast invasion
94 fails to occur or is dysfunctional, uterine spiral arterial remodeling is inadequate, and
95 placental function is suboptimal, resulting in placental hypoxia and the development
96 of pregnancy pathologies such as preeclampsia (5).

97
98 Preeclampsia affects approximately 8% of pregnancies worldwide and is recognized
99 to cause 60,000 maternal deaths and 500,000 neonatal deaths from preterm delivery
100 each year (6). This condition is characterized as early-onset (that develops before 34
101 weeks of gestation), or late-onset (develops at or after 34 weeks of gestation).

102 Early-onset preeclampsia is associated with impaired spiral artery remodeling and
103 placental ischemia and excessive release of bioactive molecules implicated in the
104 development of maternal vascular dysfunction (7, 8).

105

106 Cell-to-cell communication between the placental and maternal tissues is essential
107 for the establishment of normal pregnancy. In recent years, the role of extracellular
108 vesicles (EVs) and, in particular, small EVs called exosomes in cell-to-cell
109 communication has been recognized (9). Exosomes are nanometer-sized lipid-
110 bilayer extracellular vesicles that contain bioactive molecules, including proteins,
111 lipids, and small non-coding RNAs (e.g., miRNAs). They are released from a wide
112 range of cells (including placental cells) and are taken up by target cells to modify
113 their functions. Exosomes have been identified as important mediators in feto-
114 maternal communication (10, 11)

115
116 The concentrations of circulating exosomes in plasma are higher in pregnant
117 compared with non-pregnant women (12). Exosomes are released from placental
118 cells (e.g., syncytiotrophoblasts) into the maternal systemic circulation as early as 6
119 weeks of gestation (13), and their concentration increases through gestation (12).
120 Interestingly, higher concentrations of placental exosomes in maternal circulation are
121 associated with complications of pregnancies, such as preeclampsia (14),
122 gestational diabetes mellitus (15), intrauterine growth restriction (16), preterm birth
123 (17) and maternal obesity (18) compared with the concentrations observed during
124 normal pregnancy.

125
126 The potential role of exosomes in the development of preeclampsia has been
127 investigated by determining the effects of placenta-derived exosomes on various
128 target cells. Hypoxia increases the release of exosomes from placental cells and
129 exosomes isolated from cells incubated under low oxygen tension induce the release
130 of pro-inflammatory cytokines and decrease cell migration in their target cells (19,

131 20). Interestingly, the miRNA content of exosomes isolated from HTR-8/SVneo cells
132 (commonly used EVT model) changes in response to low oxygen tensions and
133 regulate endothelial and vascular smooth muscle cell migration (21). These data
134 support a role for exosomes from EVT in the remodeling of uterine spiral arteries
135 under both normal and pathological pregnancies (5, 21, 22).

136

137 The capacity of exosomes to induce changes in the target cells is mediated by the
138 specific delivery of bioactive molecules, such as proteins and miRNAs (23, 24).

139 Recently, using a longitudinal study design, we reported that the miRNA content
140 within exosomes changes in preeclamptic compared to normotensive pregnancies
141 (14). In addition, oxygen tension regulates the miRNA profile of EVT-derived
142 exosomes (21). The biological effects of oxygen tension on the protein profile of
143 EVT-derived exosomes, however, have yet to be described. Sammar *et al.*
144 investigated the level of expression of placental protein 13 in syncytiotrophoblast-
145 derived extracellular vesicles (STBEVs) isolated from preeclamptic and normal
146 pregnancy placental perfusate and reported low expression in preeclamptic
147 placentae (25). Tong *et al.* described a novel mechanism by which placental
148 extracellular vesicles can attenuate the pathogenesis of preeclampsia in the
149 presence of antiphospholipid antibody (aPL) that can induce the synthesis of toll-like
150 receptors on placental extracellular vesicles to increase the level of expression of
151 mitochondrial DNA in these vesicles (26). Thus, these data suggest that placenta-
152 derived EVs are involved in gene regulation, placental homeostasis, and cellular
153 function that overall reflect the placental-maternal crosstalk.

154

155 Poor placentation associated with a failed invasion of the EVT is a feature of
156 preeclampsia and is associated with hypoxia and oxidative stress. We hypothesize
157 that, in response to low oxygen tension, the EVT packages a specific set of proteins
158 in sEVs and that these released sEVs interact with endothelial cells to induce
159 inflammation and increase maternal systemic blood pressure. To test this
160 hypothesis, small EVs were isolated from a transformed extravillous trophoblast cell
161 line (HTR8/SVneo, commonly used as EVT model) cultured under different oxygen
162 tensions to mimic normal and pathological conditions. sEVs were isolated from
163 HTR8/SVneo cell-conditioned media and the protein profile was identified using
164 quantitative mass spectrometry. The effect of sEVs on the secretion of GM-CSF, IL-
165 6, IL-8, and VEGF from endothelial cells was evaluated. Finally, sEVs were injected
166 in pregnant rats and the systemic blood pressure was monitored. The results
167 obtained in this study are consistent with the hypothesis that oxygen tension
168 regulates the release and bioactivity of sEVs from HTR8/SVneo cells and that these
169 sEVs regulate maternal systemic blood pressure. Extracellular vesicles are a
170 heterogenic population of vesicles, and there is considerable debate about the
171 definition and nomenclature of the different populations of extracellular vesicles. In
172 this study, the term small extracellular vesicles (sEVs) refers to extracellular vesicles
173 with a median diameter of ~ 100 nm, which are CD63 and TSG101 positive and of
174 cup-shape morphology.

175 METHODS

176 Cell culture

177 All experimental procedures were conducted within an ISO17025 accredited
178 National Association of Testing Authorities (NATA, Australia) research facility. All
179 data were recorded within a 21 Code of Federal Regulation (CFR) part 11 compliant
180 electronic laboratory notebook (Lab Archives, Carlsbad, CA 92008, USA). The
181 project was approved by the Human Research Ethics Committees of the University
182 of Queensland and Royal Brisbane and Women Hospital (HREC/11/QRBW/342).
183 The HTR-8/SVneo cell line was kindly provided by Dr. Charles H. Graham (Queen's
184 University, Ontario, Canada). The HTR-8/SVneo cell line was established by the
185 transfection of the first-trimester trophoblasts with the Simian virus 40 large T antigen
186 (27). HTR-8/SVneo cells are commonly used as a model for extravillous trophoblast
187 function. Authentication of HTR-8/SVneo cells was performed with authentication by
188 STR DNA Profiling Analysis. HTR-8/SVneo cells were maintained in phenol red-free
189 RPMI 1640 medium supplemented with 10% heat-inactivated fetal bovine serum
190 (FBS), 1% non-essential amino acids, 1 mM sodium pyruvate, 100 U/mL penicillin,
191 and 100 mg/mL streptomycin. Cultures were maintained at 37 °C and humidified
192 under an atmosphere of 5% CO₂-balanced N₂ and either an 8% or 1% oxygen in an
193 automated PROOX 110-scaled hypoxia chamber (BioSpherics™, Lacona, NY,
194 USA). Cells were cultured in RPMI 1640 medium supplemented with 10% FBS-
195 exosomes depleted for 48h before exosome isolation. Cells were sub-cultured with
196 dissociation media, TrypLE™ Express (Life Technologies, USA), and cellular viability
197 was determined using the Trypan Blue exclusion solution and Countess® Automated
198 cell counter (Life Technologies, USA).

199

200 Isolation and characterization of small extracellular vesicles

201 Small extracellular vesicles (sEVs) were isolated from cell-conditioned media, as
202 previously described with slight modification (21). In brief, cell-conditioned media
203 was centrifuged at 2,000 x g for 10 min at 4°C (Sorvall®, high-speed
204 microcentrifuge, 90⁰ fixed rotor angle, Thermo Fisher Scientific Inc., Asheville, NC,
205 USA,). The 2,000 x g supernatant fluid was then centrifuged at 12,000 x g for 15 min
206 at 4°C (Sorvall, high-speed microcentrifuge, 90° fixed rotor angle). The resultant
207 supernatant fluid was filtered through a 0.22 µm filter (Steritop™, Millipore, Billerica,
208 MA, USA) and then subjected to size-exclusion chromatography (SEC). Briefly,
209 Pierce™ Disposable Columns, 10 mL (Thermo Scientific), were packed with 10 ml of
210 Sepharose® CL-2B (Sigma) and sorted overnight at 4°C. The packed bed was
211 equilibrated with ice-cold PBS and topped with a column filter. The 500 µl of the
212 concentrated sample was overlaid on top of the filter and followed by elution with
213 PBS. Five-hundred-microliter of 12 fractions were collected, and particle
214 concentration determined using nanoparticle tracking analysis (NAT, NanoSight).
215 High particle fractions were pooled and stored at -80°C until sEVs analysis. sEVs
216 were characterized by size distribution, the abundance of proteins associated with
217 sEVs (i.e., CD63, sc15363 [1:1000] and TSG101, EPR7130 [1:1000]) and
218 morphology using Nanoparticle Tracking Analysis (NTA), Western blot analysis and
219 electron microscopy, respectively as previously described (16). sEVs were quantified
220 using an electrochemical exosome detection method, as we previously described
221 (28). Samples were suspended in PBS and divided into several aliquots after the
222 isolation and stored immediately at -80°C. To thaw the sEVs, samples were taken
223 out from -80°C and maintained at 4°C in ice until completion of the thawing process.
224 The protein concentration and the number of vesicles were quantified immediately

225 after the isolation and also after thawing at 4°C to evaluate the stability and yield of
226 the vesicles under the storage conditions. No differences were observed in the
227 protein concentration and yield (i.e., vesicles/protein) after the thawing process. This
228 data is consistent with our previously published studies in which no significant
229 differences were observed using fresh or frozen plasma in exosome quantification,
230 exosomal marker expression, microRNA expression and protein content(13). All
231 samples were stored and thawing with the same procedure, discarding that the
232 differences observed at the endpoint experiments are due differences to stored and
233 thawing protocols.

234 **Quantitative Mass spectrometry analysis of exosomes**

235 ***In-gel Digestion.*** A local ion library was generated to use in the Sequential Window
236 Acquisition of All Theoretical mass spectra (SWATH) mass spectra analysis using
237 an in-gel digestion method. Briefly, two protein pools were prepared from exosomes
238 obtained from 8% and 1% oxygen. The samples were mixed with Bolt™ LDS
239 sample buffer (ThermoFisher), sonicated for 5 min and heated at 95°C for 5 min.
240 Samples were resolved on a Bolt™ Bis-Tris Plus polyacrylamide gel
241 (ThermoFisher) at 160 V until full separation. The gel was stained with
242 SimplyBlue™ SafeStain (ThermoFisher Scientific), and a total of 12 gel fractions
243 were excised for each pooled sample. The fractions were washed firstly with 50 mM
244 of ammonium bicarbonate/acetonitrile (ABC/ACN) followed by ACN. 50 µl of 100
245 mM DTT was added to each sample and incubated at 56°C for 30 min. DTT was
246 removed, and 70 µl of iodoacetamide (IAA) was added and incubated at room
247 temperature (RT) for 20 min. The samples were washed with 300 µl ACN and
248 incubated with 50 mM ABC/ACN for 30 min at room temperature. Then, 300 µl of
249 ACN was added and left for 2 min. ACN was removed and air-dried for 5 min. 50 µl

250 of 13 ng/μl of trypsin (Promega, Australia) in ABC was added to the alkylated gels
251 and stored on ice for 30 min. Then, 20 μl of 50 mM ABC/H₂O (v/v) was added and
252 incubated overnight at 37°C. Following overnight incubation, the supernatant
253 containing peptides was reserved. A mix of 100 μl of extraction buffer (0.25 ml 5%
254 (v/v) formic acid, 0.25 ml water and 0.5 ml ACN) was added to the gel pieces and
255 sonicated for 10 min. The resulting supernatant fluid was collected and combined
256 with the reserved supernatant fluid. The combined supernatant fluid was dried in a
257 vacuum centrifuge. The dried samples were resuspended in 200 μl 0.1% TFA.

258 **Filter Aided Sample Preparation:** For SWATH analysis, individual exosome
259 samples were processed using the Filter Aided Sample Preparation (FASP) method
260 (29). A total of 15 μg of exosome protein from each sample was reduced with an
261 equal volume of lysis buffer containing 8% SDS, 100 mM Tris, pH 7.6, and 0.2 M
262 DTT followed sonication and heating of samples at 95°C, each. Samples were
263 allowed to cool down completely before adding 8 M urea in 100 mM Tris, pH 8.5.
264 Samples were transferred into a Nanosep® filter unit with a 30K molecular weight
265 cut off and centrifuged for 10,000 g for 15 min. Then, filter units were washed with
266 400 μl of urea buffer and centrifuged for 10,000 g for 15 min. Samples were
267 alkylated by the addition of 100 μl of 50mM IAA in 8M urea buffer and incubated in
268 the dark for 20 min. The filter units were washed with 8 M urea buffer followed by
269 ABC. Proteins were digested using 0.3 μg of trypsin and incubated overnight at
270 37°C.

271 **Desalting:** The solubilized peptides from pooled and individual samples were
272 desalted using SOLAμ HRP SPE 96 well plate (Thermo Fisher Scientific) according
273 to the manufacturer's instruction. **Analysis of peptides:** Tryptic digest was loaded
274 onto a reversed-phase trap column (CHROMXP C18CL 5μm, 10 x 0.3mm;

275 Eksigent, Redwood City) and on-column wash was performed for 15 min (3 ul/min)
276 followed by peptide separation on reversed-phase CHROMXP C18CL 3 um, 120
277 A⁰, 150 x 0.075mm; (Eksigent, Redwood City) analytical column. The LC gradient
278 started with 95% mobile phase A (H₂O/ 0.1% FA), 5% B (ACN/ 0.1% FA) at 0 min
279 and increase to 10% B over for 2 min and then a 58-min linear gradient to 40% B
280 followed by 50% B for 5 min. Mobile phase B was then increased from 50% to 95 %
281 over 10 min, followed by a column wash at 95% B for 15 min and re-equilibrated
282 with 5% Buffer B for 6 min. The flow rate was kept at 250 nl/min during the entire
283 LC run. The resulting peptide samples were processed in IDA on an AB Sciex 5600
284 TripleTOF mass spectrometer with the top 18 precursor ions automatically selected
285 for fragmentation. The data obtained were combined to establish a peptide ion
286 database. For SWATH acquisition, the TripleTOF® 5600 System was configured as
287 described by Gillet at al. (30). Using an isolation width of 26 Da (25 Da of optimal
288 ion transmission efficiency and 1 Da for the window overlap), a set of 32
289 overlapping windows was constructed covering the mass range 400 to 1200 m/z.

290 **Data Processing:** To generate a local ion library, a protein database search was
291 conducted using the ProteinPilot version 4.5b Software (AB SCIEX) and the
292 Paragon™ Algorithm. The search was performed against the SwissProt Homo
293 sapiens database with a global false discovery rate (FDR) of 1% was used as the
294 threshold for the number of proteins for import. The SWATH Acquisition Microapp
295 2.0 in PeakView 2.2 (SCIEX) was used to create a spectral library file. This local
296 library was extended using the R package SwathXtend (version 2.3) (31) with a
297 published SWATH dataset of healthy human plasma (32). The extended library was
298 used for all subsequent SWATH analysis. Processing settings for the SWATH
299 Microapp: 2 peptides per protein, 3 transitions per peptide, peptide confidence

300 threshold corresponding to 1% global FDR and FDR threshold of 1% was used.
301 The retention time was then manually realigned with a minimum of 5 peptides with
302 high signal intensities and distributed along the time axis. The resulting peak area
303 for each protein after SWATH processing was exported to MarkerView 1.3.1
304 (SCIEX) for statistical analysis. The resulting data were normalized using the Total
305 Area Sums (TAS) approach. The coefficient of variation in the abundance of
306 peptides across the samples was established by comparing SWATH peptide ion
307 against the IDA library. For independent samples, *t*-tests were used to compare
308 protein expression between exosomes from cells cultured to 8% and 1% oxygen.
309 The proteins with $p < 0.05$ were considered as statistically significant.

310

311 [Ingenuity Pathway Analysis \(IPA\) and Gene set enrichment analysis \(GSEA\).](#)

312 IPA (Qiagen, Hilden, Germany) was performed to identify canonical pathways,
313 diseases and functions, and protein networks. Significantly enriched pathways for
314 the proteins and pathways were identified with the criterion p -value < 0.05 . To
315 determine the genes associated with changes in the protein in sEVs in response to
316 oxygen tensions, GSEA (version 3.0) was performed. Normalized SWATH results
317 from cells and exosomes were used in the GSEA. The protein expression data
318 were processed using the hallmark gene sets within the MSigDB database v6.2
319 with permutations set at 1000 and Signal2Noise metric for ranking genes. Default
320 values were chosen for all other parameters.

321

322 [Effect of sEVs on cytokines release from endothelial cells](#)

323 To determine the effect of exosomes on cytokine release from target cells,
324 exosomes were isolated from extravillous trophoblast cell-condition media and

325 incubated with cells under either 8% or 1% O₂. sEVs (20, 40, 80 and 100 µg
326 protein/ml equivalent to 1 to 10 x 10⁸ vesicles per ml) were then incubated with
327 endothelial cells (HMEC-1, from Lonza) in medium containing 5 mM d-glucose under
328 an atmosphere of 8% O₂ to mimic the physiological conditions for 24 h. Cytokine
329 release, defined as the accumulation of immunoreactive cytokine in cell-conditioned
330 medium, was quantified using a protein solution array assay, as previously described
331 (20).

332

333 **In vivo experiments**

334 All experimental procedures were in accordance with National Institutes of Health
335 guidelines (NIH Publication No. 85–23, revised 1996) with approval by the Animal
336 Care and Use Committee at the University of Wisconsin at Madison. All the animal
337 experiments were performed at the University of Wisconsin-Madison (USA). Timed
338 pregnant Sprague-Dawley rats (day 4 of gestation; copulation plug on day 1; Charles
339 River, Wilmington, MA) were used in the experiment. On the gestational day (GD) 6
340 (after two days of acclimatization), dams were anesthetized with 2.5% isoflurane,
341 and a flexible catheter attached to a radio transmitter (TA11PA-C10, Data Sciences,
342 and Minneapolis, MN) was inserted into the left femoral artery. After surgery, rats
343 were given housed in individual cages and allowed to recover for a week. On GD 16,
344 dams were randomly divided into 2 groups. Dams in the treatment group were
345 injected intravenously through the tail vein once daily with sEVs from 1% hypoxic
346 group (exosome protein amount-10 µg/day) for 4 days from GD 16–19. The other
347 group received sEVs form 8% normoxic group. A subset of control animals was
348 treated with saline. Blood pressures were recorded continuously from GD 14 until
349 GD 21. Blood pressure measurements obtained with a 10-s sampling period were

350 averaged and recorded every 10 minutes, 24 hours a day using the software
351 (Dataquest 4.0) provided by the manufacturer. All acquired blood pressure, and
352 heart rate data were averaged into 12-hour blocks paralleling the light-dark cycle.

353

354 **Statistical analysis**

355 All data are presented as mean \pm SEM and calculated using Graph Pad Prism (La
356 Jolla, CA). Repeated measures ANOVA (treatment and time as factors) with a
357 Bonferroni post hoc were used for comparisons of blood pressures between the
358 hypoxic (1% oxygen) and control (8% oxygen) groups. Statistical significance was
359 defined as $p < 0.05$.

360 RESULTS

361 Isolation of sEVs from extravillous trophoblasts

362 sEVs were isolated from HTR-8/SVneo cell-conditioned media and enriched using
363 differential centrifugation and SEC (Figure 1A). The NTA analysis identified vesicles
364 with a diameter between 50 to 150 nm, with enrichment of vesicles of around 100 nm
365 (Figure 1B and C), consistent with sEVs. Vesicles were positive for proteins known to
366 enriched in sEVs, *i.e.*, CD63 and TSG101 (Figure 1D). There were no differences in
367 exosome size distribution and abundance of sEVs-associated protein markers
368 between sEVs isolated from EVT cultured under normoxic and hypoxic conditions,
369 indicating that hypoxia does not impact upon the size distribution of sEVs. The
370 morphology and size of the sEVs were confirmed by electron microscopy (Figure
371 1E). Interestingly, the levels of EVT-derived sEVs from cells cultured under hypoxic
372 conditions were around 3-fold higher ($p < 0.05$) compared with the values observed in
373 normoxic conditions (Figure 2A).

374

375 Proteomic contents of extravillous trophoblast sEVs

376 Information-dependent acquisition (IDA) and SWATH profile were generated from
377 sEVs from HTR-8/SVneo cells cultured at 1% (hypoxic) or 8% (normoxic) oxygen
378 concentrations. The IDA library was used to identify peptide ions that were present in
379 SWATH ion profiles. Proteins were identified and quantified by comparing SWATH-
380 generated peptide ion profiles for each sample against the IDA library (PeakView).
381 IDA of mass spectra from sEVs samples was initially performed and identified 727
382 total proteins (Table S1) and analyzed using IDA and SWATH. To evaluate whether
383 hypoxia changes the protein profile within sEVs from HTR-8/SVneo cells, we

384 analyzed data using an unsupervised principal component analysis (PCA) with
385 Qlucore Omics Explorer. With the first three PCA components explaining >90% of
386 the total variance, the generated PCA plot revealed that the sEVs from hypoxic and
387 normoxic groups had distinct protein contents (Figure 2B). The variation in the
388 relative abundance of exosomal proteins between sEVs from hypoxic and normoxic
389 cell lines was established by comparison with the SWATH profile against the IDA
390 library and presented as a volcano plot (Figure 2C). A total of 507 statistically
391 significant proteins (206 up- and 301 down-regulated) were differentially expressed.
392 Among all the proteins, alpha-2 macroglobulin, alpha-fetoprotein, apolipoproteins A1
393 and E, chaperonin, gelsolin, heat shock proteins (Hsp90, Hsp70, Hsp60, and
394 Hsp10), inter alpha trypsin inhibitor, gamma-glutamyl transferase, lactotransferrin,
395 serpin, thrombospondin, tubulin, vitrin, vitronectin, annexin family of proteins,
396 fibronectin, histone, haptoglobin, syndecan-1, galectin 3 binding protein,
397 glyceraldehyde 3 phosphate dehydrogenase, and alpha 2 HS glycoprotein were
398 identified that are likely to be associated with preeclampsia pathogenesis.

399
400 To investigate the potential functions of the differentially expressed proteins,
401 pathway analysis of the exosomal proteomic profile was performed. The top
402 canonical pathways identified by IPA are presented in the Figure 3A; with the most
403 significant difference in the sEVs protein profiles between these groups were
404 associated with Eukaryotic Initiation Factor 2 (EIF2; a signaling pathway that
405 activates vascular endothelial growth factor, VEGF signaling, and with glucocorticoid
406 receptor signaling pathway). Interestingly, the majority of the pathways were
407 associated with inflammation, and the top 25 canonical pathways with the common
408 genes (network/overlap) are presented in Figure 3B. Many of the differentially

409 expressed genes are present in multiple pathways related to inflammation. Finally,
410 GSEA of the total protein profile revealed several gene sets that were significantly
411 enriched in sEVs derived from hypoxic compared with normoxic cells. This is
412 illustrated by the normalized enrichment score. There was an enrichment of proteins
413 involved in MYC targets, hypoxia, and epithelial to mesenchymal transition
414 suggesting that these biological processes might be regulated by the hypoxic sEVs
415 (Figure 3C).

416

417 **Effect of HTR-8/SVneo cells-derived sEVs on cytokines releases from** 418 **endothelial cells**

419 The effect of hypoxic and normoxic sEVs on the release of IL-6, IL-8, VEGF, and
420 GM-CSF from endothelial cells is presented in Figure 4. sEVs derived from hypoxic
421 EVT dose-dependently increased ($p < 0.05$) the release of all cytokines from
422 endothelial cells when compared to controls (without sEVs) or sEVs from cells
423 cultured at 8% oxygen (normoxic control).

424

425 **Effect of EVT-derived exosome in systemic blood pressure in pregnant rats.**

426 The mean litter size and maternal weights were similar between hypoxic (1%
427 oxygen) and control (8% oxygen) groups. Fetal weights (8% O₂: 2.59 ± 0.06 g; 1%
428 O₂: 2.47 ± 0.05 g), placental weights on GD 21 (1%: 0.48 ± 0.09 g; 8%: 0.50 ± 0.05 g)
429 were comparable between the two groups. Rats are nocturnal animals, and
430 continuous monitoring of blood pressure by telemetry revealed a characteristic
431 circadian pattern with higher arterial pressure and heart rate values during the dark
432 cycle (active phase) compared to the light cycle. In animals injected with normoxic
433 sEVs, MAP progressively decreased from GD 16 and reached a nadir on GD21,

434 which was comparable to the MAP in the saline-injected group. Pregnant rats
435 injected with hypoxic sEVs had significantly higher MAP starting from GD18 to GD21
436 compared to the respective time point in the control group (Figure 5A; n=6 rats in
437 each group; $P < 0.05$). The changes in MAP correlated with a significant increase in
438 systolic blood pressures in the hypoxic compared to the control group (Figure 5B; n=
439 6 rats in each group). The diastolic blood pressure increased only in the later part of
440 gestation (i.e., GD 20-21) in the hypoxic compared to the control group (Figure 5C;
441 n=6 rats in each group). No differences in heart rate were observed between the
442 hypoxic and control groups (Figure 6; n=6 rats in each group).

443 DISCUSSION

444 The data obtained in this study are consistent with the hypothesis that the protein
445 content of EVT sEVs is programmed by low oxygen tension to be pro-inflammatory
446 (i.e., increasing the release of the IL-6, IL-8, VEGF and CS-GMS from target cells)
447 and to promote hypertension.

448 The bioinformatic analysis revealed that in normoxic (8% oxygen) conditions, the
449 proteins in EVT sEVs are associated with EIF2 signaling that activates the VEGF
450 signaling pathway. VEGF is a protein mediator that is synthesized and secreted by
451 placental macrophages. VEGF binds as a ligand with the soluble fms-like tyrosine
452 kinase (sFLT-1) receptor (also described as VEGF receptor 1) expressed on the
453 surface of vascular endothelial and smooth muscle cells (33). It also binds with the
454 kinase insert domain (KDR) receptor (also described as VEGF receptor 2), which is
455 expressed only on the surface of vascular endothelial cells (33). Activation of these
456 pathways assists in increasing endothelial cell permeability, migration, proliferation,
457 and survival, ultimately leading to proper angiogenesis of the fetoplacental vascular
458 tree and contributing to adequate trophoblast development and placental perfusion

459 (34). VEGF also mediates vasodilatation and increases vessel permeability via the
460 release of nitric oxide from the uterine arterial endothelial cells in pregnancy (35). In
461 preeclampsia, however, maladaptation occurs due to the altered concentrations of
462 VEGF and PlGF, augmented placental secretion of sFLT-1 and soluble endoglin
463 (sEng), polymorphism in the endothelial nitric oxide gene and reduced
464 bioavailability of nitric oxide secondary to oxidative stress (36). The consequences
465 are inappropriate angiogenesis, endothelial dysfunction and vasoconstriction leading
466 to inadequate placental perfusion to the fetus and maternal hypertension.

467

468 A recent study reported that the gene regulating sFLT-1 receptor (that binds with
469 VEGF) is polymorphic and that some variants increase susceptibility to preeclampsia
470 (37). Virtanen *et al.*, found that the concentrations of angiogenic proteins (VEGF and
471 PlGF) in serum collected from women during the third trimester of uncomplicated
472 pregnancies are increased and that they stimulate angiogenesis. These angiogenic
473 factors were found to be decreased in preeclamptic serum, and they also inhibited
474 tubule formation (38). The findings of our study are consistent with previous data
475 suggesting that VEGF signaling and placental vasculogenesis are regulated by
476 hypoxia (39).

477

478 A hypoxic environment (1% oxygen tension for culture) also promotes the packaging
479 of EVT sEVs with proteins involved in glucocorticoid receptor signaling.

480 Glucocorticoids (GC) are steroid hormones that are secreted predominantly from the
481 adrenal gland. These hormones exert diverse effects on vascular function and have
482 an anti-angiogenic effect (40). Ozmen *et al.* studied the effects of GC on human
483 umbilical vein endothelial cells (HUVEC), where they observed increased expression

484 of VEGF and VEGFR1 proteins and decreased expression of VEGFR2 protein when
485 HUVECs were treated with GCs (40). Recently, we have reported that the differential
486 expression of exosomal miRNAs in maternal plasma in term and preterm birth are
487 associated with GC receptor signaling (41).

488 The concentration of maternal cortisol increases with gestation and is significantly
489 correlated with blood pressure rise during pregnancy (42). The GC receptor gene is
490 located on chromosome 5q and encodes a nuclear transcription factor that mediates
491 GC receptor signaling Polymorphism in the (GC) receptor is associated with the
492 development of hypertension (43). Interestingly, genetic variants of stratin, a protein
493 that interacts with the steroid (GC) receptors, is associated with salt-sensitive blood
494 pressure regulation in mice (44). Moreover, the peripheral blood-derived mixed
495 population of exosomal microRNAs can regulate systolic blood pressure in older
496 individuals (45). Placental trophoblast derived exosomal micro RNAs are associated
497 with maternal-fetal immune interaction and the physiologic consequences of
498 placental-maternal communication in a murine model (46). Another study observed
499 that human umbilical cord mesenchymal stem cell-derived sEVs improves the
500 placental tissue morphology in the pregnant rat by inhibiting trophoblast apoptosis
501 and promoting placental angiogenesis (47). These reports support our hypothesis
502 that the proteins encapsulated in sEVs isolated from EVT's cultured under hypoxia
503 can prevent the decrease in blood pressure observed in normal pregnancy
504 mimicking preeclamptic symptoms in an in-vivo model- pregnant rats. This lack of a
505 pregnancy-related fall in blood pressure is considered as a cardinal feature of
506 preeclampsia (48), which is also observed in other rat models of preeclampsia (49,
507 50). This suggests that the mechanisms controlling blood pressure during pregnancy
508 are perturbed by proteins encapsulated in sEVs isolated from EVT's cultured under

509 hypoxia. The lack of impact on fetal growth and number in this study suggests that
510 this could be a mild model of preeclampsia. Further studies should examine if higher
511 exosomes concentrations in pregnant rats could negatively impact fetal weight
512 producing a severe form of preeclampsia. The patterns of exosomal protein
513 expression and VEGF and GRS signaling pathways seen in the hypoxic and control
514 groups may give some insights into explaining the hypertensive effect of hypoxia
515 treated EVT sEV proteins.

516 In this study, we used HTR8/SVneo cell line as EVT model, which is frequently used
517 as a model of physiologically invasive extravillous trophoblast. Previous studies have
518 demonstrated that HTR8/SVneo express KR7, CG, CGR, and HLG (51) consistent
519 with proteins identified in primary EVT. We have previously established that EVT-
520 derived exosomes carry HLA-G (21). However, other studies have reported whether
521 HTR-8/SVneo cells contain a mix of cell populations that differs compared with
522 primary EVT. For example, Abou-Kheir *et al.*, showed that the HTR-8/SVneo cells
523 contained a heterogeneous population of cells including trophoblast and
524 mesenchymal/stromal cells (52). In comparison to other placental cell lines, the
525 abundance of epithelial markers such as cytokeratin 7 (KR7) and e-cadherin was
526 silenced in HTR-8/SVneo cells (52-54) while a higher abundance of vimentin (a
527 marker of epithelial to mesenchymal transition) was observed (52-55). Likewise,
528 Takao *et al.*, observed low expression of HLA-G and integrin alpha-V/beta-3 (56),
529 which are known primary EVT (epithelial) markers (57-59). Furthermore, genome-
530 wide gene expression profiles showed that the molecular signature of HTR8/SVneo
531 cells was vastly different from that of primary EVTs (60). Therefore, results obtained
532 from HTR-8/SVneo cells must be further verified using the appropriate primary EVT
533 cells.

534
535
536
537
538
539
540
541
542
543
544
545
546
547
548
549
550
551
552
553
554
555
556
557
558

Based on the data obtained, we suggest that hypoxia alters the content of EVT sEVs and that these changes contribute to the physiopathology of preeclampsia. The changes in protein and miRNA expression promote an inflammatory environment within uterine spiral arteries and cause hypertension during pregnancy. These changes are likely to occur in pregnancies characterized by compromised placental perfusion and ischemia (expressed as preeclampsia and intrauterine growth restriction) as an adaptive response aiming to improve placentation.

Authors Disclosure Statement: The authors have no conflict of interest to declare.

Funding Statement: Lions Medical Research Foundation, National Health and Medical Research Council (NHMRC; 1114013), Fondo Nacional de Desarrollo Científico y Tecnológico (FONDECYT 1170809), and National Institutes of Health (NIH; HL134779).

Author's contributions: C.S., S.D. conceived and designed the study. S.K., and C.S. designed the in vivo experiments. S.S., A.L., K.S-R., M.S., Y.Y., and J.M. performed the experiments. S.D. and C.S. wrote the manuscript. C.S., G.R., S.K., and J.H. edited the manuscript. All authors reviewed/edited the manuscript and approved the final version. C.S. is the guarantor of this work and, as such, had full access to all the data in the study and takes responsibility for the integrity of the data and the accuracy of the data analysis.

559

560

561 **Reference:**

- 562 1. Holcberg G, D. S, A. B. Implantation, Physiology of Placentation. In: al. BAe, editor.
563 Recurrent Pregnancy Loss. Switzerland: Springer International Publishing Switzerland; 2016.
- 564 2. Schoots MH, Gordijn SJ, Scherjon SA, van Goor H, Hillebrands J-L. Oxidative stress in
565 placental pathology. *Placenta*. 2018;69:153-61.
- 566 3. James JL, Saghian R, Perwick R, Clark AR. Trophoblast plugs: impact on utero-
567 placental haemodynamics and spiral artery remodelling. *Human reproduction (Oxford,*
568 *England)*. 2018.
- 569 4. Moser G, Huppertz B. Implantation and extravillous trophoblast invasion: From rare
570 archival specimens to modern biobanking. *Placenta*. 2017;56:19-26.
- 571 5. Salomon C, Yee SW, Mitchell MD, Rice GE. The possible role of extravillous
572 trophoblast-derived exosomes on the uterine spiral arterial remodeling under both normal
573 and pathological conditions. *Biomed Res Int*. 2014;2014:693157.
- 574 6. Marshall SA, Hannan NJ, Jelinic M, Nguyen TPH, Girling JE, Parry LJ. Animal models of
575 preeclampsia: Translational failings and why. *American Journal of Physiology - Regulatory*
576 *Integrative and Comparative Physiology*. 2018;314(4):R499-R508.
- 577 7. Conrad KP, Benyo DF. Placental cytokines and the pathogenesis of preeclampsia.
578 *American journal of reproductive immunology (New York, NY : 1989)*. 1997;37(3):240-9.
- 579 8. Tannetta D, Masliukaite I, Vatish M, Redman C, Sargent I. Update of
580 syncytiotrophoblast derived extracellular vesicles in normal pregnancy and preeclampsia.
581 *Journal of reproductive immunology*. 2016.
- 582 9. Thery C, Zitvogel L, Amigorena S. Exosomes: composition, biogenesis and function.
583 *Nat Rev Immunol*. 2002;2(8):569-79.
- 584 10. Mitchell MD, Peiris HN, Kobayashi M, Koh YQ, Duncombe G, Illanes SE, et al.
585 Placental exosomes in normal and complicated pregnancy. *Am J Obstet Gynecol*. 2015;213(4
586 *Suppl*):S173-81.
- 587 11. Adam S, Elfeky O, Kinhal V, Dutta S, Lai A, Jayabalan N, et al. Review: Fetal-maternal
588 communication via extracellular vesicles - Implications for complications of pregnancies.
589 *Placenta*. 2017;54:83-8.
- 590 12. Salomon C, Torres MJ, Kobayashi M, Scholz-Romero K, Sobrevia L, Dobierzewska A,
591 et al. A gestational profile of placental exosomes in maternal plasma and their effects on
592 endothelial cell migration. *PLoS One*. 2014;9(6):e98667.
- 593 13. Sarker S, Scholz-Romero K, Perez A, Illanes SE, Mitchell MD, Rice GE, et al. Placenta-
594 derived exosomes continuously increase in maternal circulation over the first trimester of
595 pregnancy. *J Transl Med*. 2014;12:204.
- 596 14. Salomon C, Guanzon D, Scholz-Romero K, Longo S, Correa P, Illanes SE, et al.
597 Placental Exosomes as Early Biomarker of Preeclampsia: Potential Role of Exosomal
598 MicroRNAs Across Gestation. *J Clin Endocrinol Metab*. 2017;102(9):3182-94.
- 599 15. Salomon C, Scholz-Romero K, Sarker S, Sweeney E, Kobayashi M, Correa P, et al.
600 Gestational Diabetes Mellitus Is Associated With Changes in the Concentration and
601 Bioactivity of Placenta-Derived Exosomes in Maternal Circulation Across Gestation.
602 *Diabetes*. 2016;65(3):598-609.

- 603 16. Miranda J, Paules C, Nair S, Lai A, Palma C, Scholz-Romero K, et al. Placental
604 exosomes profile in maternal and fetal circulation in intrauterine growth restriction - Liquid
605 biopsies to monitoring fetal growth. *Placenta*. 2018;64:34-43.
- 606 17. Menon R, Dixon CL, Sheller-Miller S, Fortunato SJ, Saade GR, Palma C, et al.
607 Quantitative Proteomics by SWATH-MS of Maternal Plasma Exosomes Determine Pathways
608 Associated With Term and Preterm Birth. *Endocrinology*. 2019;160(3):639-50.
- 609 18. Elfeky O, Longo S, Lai A, Rice GE, Salomon C. Influence of maternal BMI on the
610 exosomal profile during gestation and their role on maternal systemic inflammation.
611 *Placenta*. 2017;50:60-9.
- 612 19. Truong G, Guanzon D, Kinhal V, Elfeky O, Lai A, Longo S, et al. Oxygen tension
613 regulates the miRNA profile and bioactivity of exosomes released from extravillous
614 trophoblast cells – Liquid biopsies for monitoring complications of pregnancy. *PloS one*.
615 2017;12(3):e0174514.
- 616 20. Rice GE, Scholz-Romero K, Sweeney E, Peiris H, Kobayashi M, Duncombe G, et al. The
617 Effect of Glucose on the Release and Bioactivity of Exosomes From First Trimester
618 Trophoblast Cells. *The Journal of clinical endocrinology and metabolism*.
619 2015;100(10):E1280-8.
- 620 21. Truong G, Guanzon D, Kinhal V, Elfeky O, Lai A, Longo S, et al. Oxygen tension
621 regulates the miRNA profile and bioactivity of exosomes released from extravillous
622 trophoblast cells - Liquid biopsies for monitoring complications of pregnancy. *PLoS One*.
623 2017;12(3):e0174514.
- 624 22. Salomon C, Yee S, Scholz-Romero K, Kobayashi M, Vaswani K, Kvaskoff D, et al.
625 Extravillous trophoblast cells-derived exosomes promote vascular smooth muscle cell
626 migration. *Front Pharmacol*. 2014;5:175.
- 627 23. Zhang D, Lee H, Zhu Z, Minhas JK, Jin Y. Enrichment of selective miRNAs in exosomes
628 and delivery of exosomal miRNAs in vitro and in vivo. *Am J Physiol Lung Cell Mol Physiol*.
629 2017;312(1):L110-L21.
- 630 24. Kramer-Albers EM. Ticket to Ride: Targeting Proteins to Exosomes for Brain Delivery.
631 *Mol Ther*. 2017;25(6):1264-6.
- 632 25. Sammar M, Dragovic R, Meiri H, Vatish M, Sharabi-Nov A, Sargent I, et al. Reduced
633 placental protein 13 (PP13) in placental derived syncytiotrophoblast extracellular vesicles in
634 preeclampsia - A novel tool to study the impaired cargo transmission of the placenta to the
635 maternal organs. *Placenta*. 2018;66:17-25.
- 636 26. Tong M, Johansson C, Xiao F, Stone PR, James JL, Chen Q, et al. Antiphospholipid
637 antibodies increase the levels of mitochondrial DNA in placental extracellular vesicles:
638 Alarmin-g for preeclampsia. *Sci Rep*. 2017;7(1):16556.
- 639 27. Graham CH, Hawley TS, Hawley RG, MacDougall JR, Kerbel RS, Khoo N, et al.
640 Establishment and characterization of first trimester human trophoblast cells with extended
641 lifespan. *Exp Cell Res*. 1993;206(2):204-11.
- 642 28. Boriachek K, Masud MK, Palma C, Phan HP, Yamauchi Y, Hossain MSA, et al. Avoiding
643 Pre-Isolation Step in Exosome Analysis: Direct Isolation and Sensitive Detection of Exosomes
644 Using Gold-Loaded Nanoporous Ferric Oxide Nanozymes. *Anal Chem*. 2019;91(6):3827-34.
- 645 29. Barr SM, Walker BR, Morton NM, Norman JE. Pro-inflammatory gene mRNA levels
646 are elevated in subcutaneous but not visceral adipose tissue in obese pregnant women.
647 *BJOG*. 2011;118(8):1008-9.
- 648 30. Catalano PM, Ehrenberg HM. The short- and long-term implications of maternal
649 obesity on the mother and her offspring. *Bjog*. 2006;113(10):1126-33.

- 650 31. Wu J, Pascovici D. SwathXtend: SWATH extended library generation and statistical
651 data analysis. 2.3.0. ed2018. p. R package version 2.3.0.
- 652 32. Bjelosevic S, Pascovici D, Ping H, Karlaftis V, Zaw T, Song X, et al. Quantitative Age-
653 specific Variability of Plasma Proteins in Healthy Neonates, Children and Adults. *Molecular &*
654 *cellular proteomics : MCP*. 2017;*16*(5):924-35.
- 655 33. Ji S, Xin H, Li Y, Su EJ. FMS-like tyrosine kinase 1 (FLT1) is a key regulator of
656 fetoplacental endothelial cell migration and angiogenesis. *Placenta*. 2018;*70*:7-14.
- 657 34. Pavlov OV, Niauri DA, Selutin AV, Selkov SA. Coordinated expression of TNFalpha-
658 and VEGF-mediated signaling components by placental macrophages in early and late
659 pregnancy. *Placenta*. 2016;*42*:28-36.
- 660 35. Zhang HH, Chen JC, Sheibani L, Lechuga TJ, Chen DB. Pregnancy Augments VEGF-
661 Stimulated In Vitro Angiogenesis and Vasodilator (NO and H2S) Production in Human
662 Uterine Artery Endothelial Cells. *The Journal of clinical endocrinology and metabolism*.
663 2017;*102*(7):2382-93.
- 664 36. Osol G, Ko NL, Mandala M. Altered Endothelial Nitric Oxide Signaling as a Paradigm
665 for Maternal Vascular Maladaptation in Preeclampsia. *Current hypertension reports*.
666 2017;*19*(10):82.
- 667 37. Amin-Beidokhti M, Gholami M, Abedin-Do A, Pirjani R, Sadeghi H, Karamoddin F, et
668 al. An intron variant in the FLT1 gene increases the risk of preeclampsia in Iranian women.
669 *Clinical and experimental hypertension (New York, NY : 1993)*. 2018:1-5.
- 670 38. Virtanen A, Huttala O, Tihtonen K, Toimela T, Heinonen T, Uotila J. Angiogenic
671 capacity in pre-eclampsia and uncomplicated pregnancy estimated by assay of angiogenic
672 proteins and an in vitro vasculogenesis/angiogenesis test. *Angiogenesis*. 2019;*22*(1):67-74.
- 673 39. Zafer E, Yenisey C, Kurek Eken M, Ozdemir E, Kurt Omurlu I, Yuksel H. Second
674 trimester maternal serum-amniotic fluid nitric oxide and vascular endothelial growth factor
675 levels in relation to uterine artery Doppler indices in pregnancies with normal outcome.
676 *Journal of obstetrics and gynaecology : the journal of the Institute of Obstetrics and*
677 *Gynaecology*. 2018;*38*(8):1088-92.
- 678 40. Ozmen A, Unek G, Kipmen-Korgun D, Mendilcioglu I, Sanhal C, Sakinci M, et al.
679 Glucocorticoid effects on angiogenesis are associated with mTOR pathway activity.
680 *Biotechnic & histochemistry : official publication of the Biological Stain Commission*.
681 2016;*91*(4):296-306.
- 682 41. Menon R, Debnath C, Lai A, Guanzon D, Bhatnagar S, Kshetrapal PK, et al. Circulating
683 Exosomal miRNA Profile During Term and Preterm Birth Pregnancies: A Longitudinal Study.
684 *Endocrinology*. 2019;*160*(2):249-75.
- 685 42. Bärebring L, O'Connell M, Winkvist A, Johannsson G, Augustin H. Serum cortisol and
686 vitamin D status are independently associated with blood pressure in pregnancy. *Journal of*
687 *Steroid Biochemistry and Molecular Biology*. 2019.
- 688 43. Chung CC, Shimmin L, Natarajan S, Hanis CL, Boerwinkle E, Hixson JE. Glucocorticoid
689 receptor gene variant in the 3' untranslated region is associated with multiple measures of
690 blood pressure. *The Journal of clinical endocrinology and metabolism*. 2009;*94*(1):268-76.
- 691 44. Garza AE, Rariy CM, Sun B, Williams J, Lasky-Su J, Baudrand R, et al. Variants in
692 striatin gene are associated with salt-sensitive blood pressure in mice and humans.
693 *Hypertension (Dallas, Tex : 1979)*. 2015;*65*(1):211-7.
- 694 45. Rodosthenous RS, Kloog I, Colicino E, Zhong J, Herrera LA, Vokonas P, et al.
695 Extracellular vesicle-enriched microRNAs interact in the association between long-term

696 particulate matter and blood pressure in elderly men. *Environmental research*.
697 2018;167:640-9.

698 46. Stefanski AL, Martinez N, Peterson LK, Callahan TJ, Treacy E, Luck M, et al. Murine
699 trophoblast-derived and pregnancy-associated exosome-enriched extracellular vesicle
700 microRNAs: Implications for placenta driven effects on maternal physiology. *PLoS one*.
701 2019;14(2):e0210675.

702 47. Xiong ZH, Wei J, Lu MQ, Jin MY, Geng HL. Protective effect of human umbilical cord
703 mesenchymal stem cell exosomes on preserving the morphology and angiogenesis of
704 placenta in rats with preeclampsia. *Biomedicine & pharmacotherapy = Biomedecine &
705 pharmacotherapie*. 2018;105:1240-7.

706 48. Ishikuro M, Obara T, Metoki H, Ohkubo T, Yaegashi N, Kuriyama S, et al. Blood
707 pressure changes during pregnancy. *Hypertens Res*. 2012;35(5):563-4; author reply 34.

708 49. Chinnathambi V, Balakrishnan M, Ramadoss J, Yallampalli C, Sathishkumar K.
709 Testosterone alters maternal vascular adaptations: role of the endothelial NO system.
710 *Hypertension*. 2013;61(3):647-54.

711 50. Isler CM, Bennett WA, Rinewalt AN, Cockrell KL, Martin JN, Jr., Morrison JC, et al.
712 Evaluation of a rat model of preeclampsia for HELLP syndrome characteristics. *J Soc Gynecol
713 Investig*. 2003;10(3):151-3.

714 51. Hannan NJ, Paiva P, Dimitriadis E, Salamonsen LA. Models for study of human
715 embryo implantation: choice of cell lines? *Biol Reprod*. 2010;82(2):235-45.

716 52. Abou-Kheir W, Barrak J, Hadadeh O, Daoud G. HTR-8/SVneo cell line contains a
717 mixed population of cells. *Placenta*. 2017;50:1-7.

718 53. Chen Y, Wang K, Leach R. 5-Aza-dC treatment induces mesenchymal-to-epithelial
719 transition in 1st trimester trophoblast cell line HTR8/SVneo. *Biochemical and Biophysical
720 Research Communications*. 2013;432(1):116-22.

721 54. Daoud G, Barrak J, Abou-Kheir W. Assessment Of Different Trophoblast Cell Lines As
722 In Vitro Models For Placental Development. *The FASEB Journal*. 2016;30(1
723 Supplement):1247.18-.18.

724 55. DaSilva-Arnold S, James JL, Al-Khan A, Zamudio S, Illsley NP. Differentiation of first
725 trimester cytotrophoblast to extravillous trophoblast involves an epithelial-mesenchymal
726 transition. *Placenta*. 36(12):1412-8.

727 56. Takao T, Asanoma K, Kato K, Fukushima K, Tsunematsu R, Hirakawa T, et al. Isolation
728 and characterization of human trophoblast side-population (SP) cells in primary villous
729 cytotrophoblasts and HTR-8/SVneo cell line. *PLoS one*. 2011;6(7):e21990.

730 57. Ellis SA, Palmer MS, McMichael AJ. Human trophoblast and the choriocarcinoma cell
731 line BeWo express a truncated HLA Class I molecule. *Journal of immunology (Baltimore, Md
732 : 1950)*. 1990;144(2):731-5.

733 58. Kabir-Salmani M, Shiokawa S, Akimoto Y, Sakai K, Nagamatsu S, Sakai K, et al.
734 Alphavbeta3 integrin signaling pathway is involved in insulin-like growth factor I-stimulated
735 human extravillous trophoblast cell migration. *Endocrinology*. 2003;144(4):1620-30.

736 59. Kovats S, Main EK, Librach C, Stubblebine M, Fisher SJ, DeMars R. A class I antigen,
737 HLA-G, expressed in human trophoblasts. *Science (New York, NY)*. 1990;248(4952):220-3.

738 60. Bilban M, Tauber S, Haslinger P, Pollheimer J, Saleh L, Pehamberger H, et al.
739 Trophoblast invasion: Assessment of cellular models using gene expression signatures.
740 *Placenta*. 2010;31(11):989-96.

741

742 Figures

743

744 **Figure 1. Characterization of sEVs isolated from HTR-8/SVneo cells.** sEVs were
745 isolated from cell-conditioned media by differential and ultracentrifugation, followed
746 by size exclusion chromatography. (A) Flow chart for the exosome isolation and
747 enrichment procedure (B and C) Representative size distribution of sEVs in NTA of
748 sEVs isolated from cells cultured at 1% oxygen and 8% oxygen, respectively. (D)
749 Representative Western blot for exosome enriched marker CD63 and TSG101. (E)
750 Electron micrograph of sEVs-exo. In E, scale = 100nm.

751

752 **Figure 2. Comparison of protein enrichment in sEVs from HTR-8/SVneo cells**
753 **cultured at different oxygen tensions.** (A) Quantification of sEVs particles from
754 HTR-8/SVneo cells cultured under 1% or 8% oxygen presented as the normalized
755 number of particles/ 10^6 cells/48 h using an electrochemical exosome detection
756 method based on biotinylated anti-CD9 (Abcam) onto the surface of a streptavidin-
757 coated screen-printed carbon electrode (SPCE-STR). (B) principal component
758 analysis (PCA) plot of the protein profile within sEVs from extravillous trophoblasts
759 (exo-EVT) cultured at 1% and 8%. (C) Volcano plot showing differentially expressed
760 protein in the hypoxic sEVs compared to normoxic sEVs-exo. The horizontal axis
761 represents the \log_2 of fold change and the vertical axis represents *p-value*. The
762 horizontal dotted line shows $p=0.05$. Each blue dot represents a protein with blue
763 dots on the right above the dashed line are proteins upregulated while on the left are
764 downregulated in hypoxic sEVs.

765

766 **Figure 3. Bioinformatic analysis of sEVs.** (A) IPA canonical pathway analysis of
767 the protein content within sEVs from hypoxic compared with normoxic. (B) The top
768 25 canonical pathways selected for finding the genes common in more than one
769 canonical pathway (overlap). (C) sEVs protein signatures were analyzed by GSEA
770 using the gene sets (GSE) derived from HTR-8/SVneo cells cultured under 8% and
771 1% oxygen.

772

773

774 **Figure 4. Effect of sEVs on cytokines secretion from endothelial cells.** The
775 concentration of GM-CSF, IL-6, IL-8, and VEGF were quantified in sEVs and
776 endothelial cell-conditioned media using an ELISA kit. sEVs were isolated from HTR-
777 8/SVneo cells cultured at 8% and 1% oxygen and the concentration of IL-6 (A), IL-8
778 (B), VEGF (C), and GM-CSF (D), were quantified in sEVs. Data represents n=4 well
779 for each point (6 different experiments in duplicate). Values are mean \pm SEM.

780

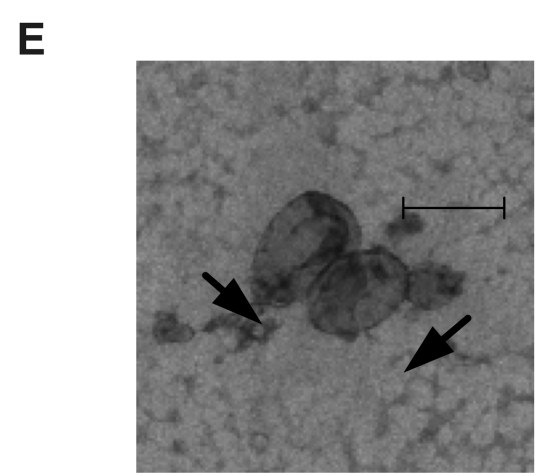
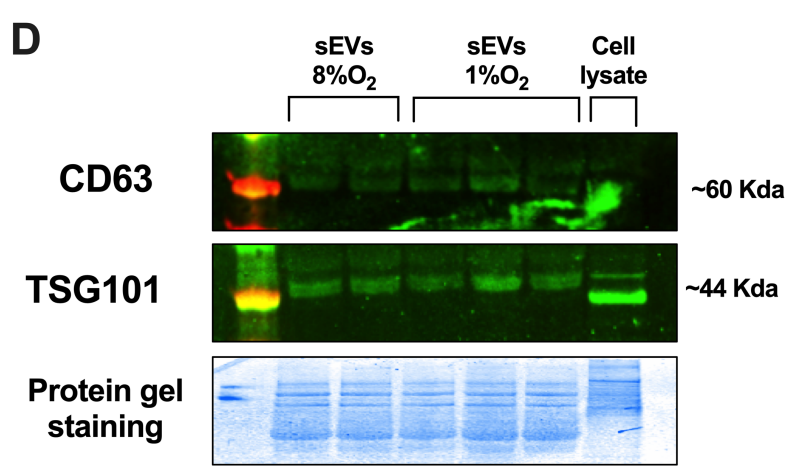
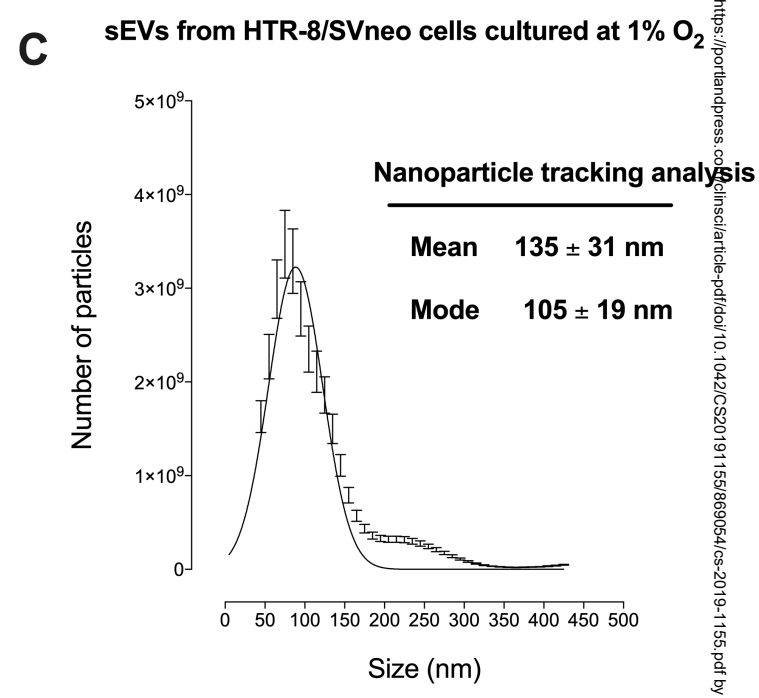
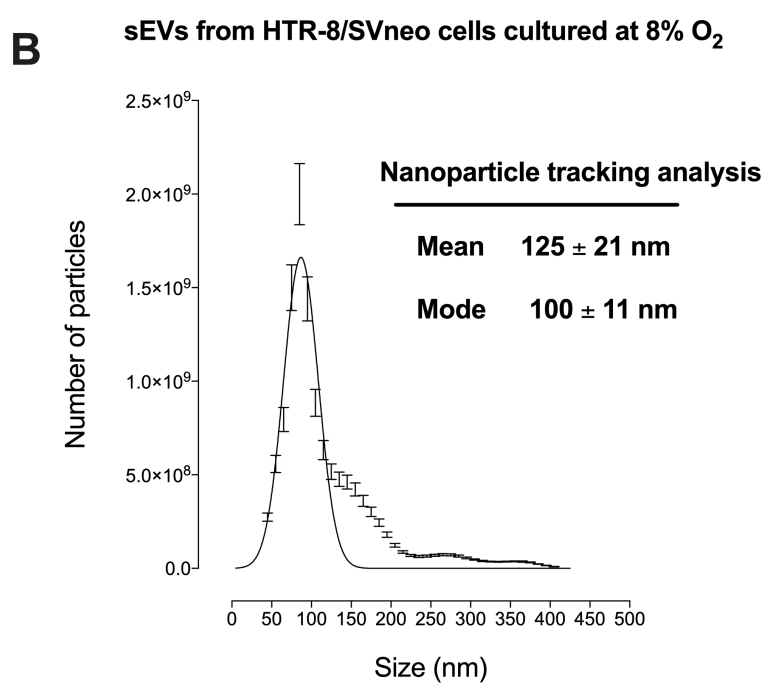
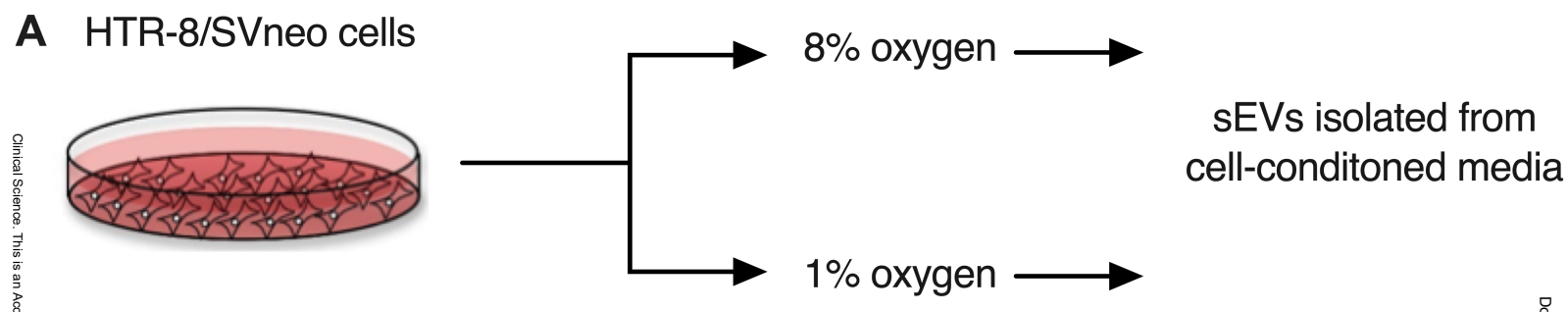
781

782 **Figure 5. Mean arterial, systolic, and diastolic pressure in pregnant rats treated**
783 **with 1% and 8% hypoxic sEVs.** (A) Mean blood pressure was continuously
784 monitored *via* telemetry catheters in the femoral artery from gestational day (GD) 14
785 until GD 21. Mean blood pressures are presented in 12-h intervals showing circadian
786 variation; dark periods are shaded. Data represent the mean \pm SEM of
787 measurements in 6 rats in each group. * $p \leq 0.05$ 1% vs 8% hypoxic group. (B and C)
788 Mean systolic and diastolic pressure were continuously monitored *via* telemetry
789 catheters in the femoral artery from gestational day (GD) 14 until GD 21. Mean
790 systolic and diastolic pressures are presented in 12-h intervals showing circadian
791 variation; nighttime periods are shaded. Data points represent the mean \pm SEM of
792 measurements in 6 rats in each group. * $P \leq 0.05$ vs 8% hypoxic group.

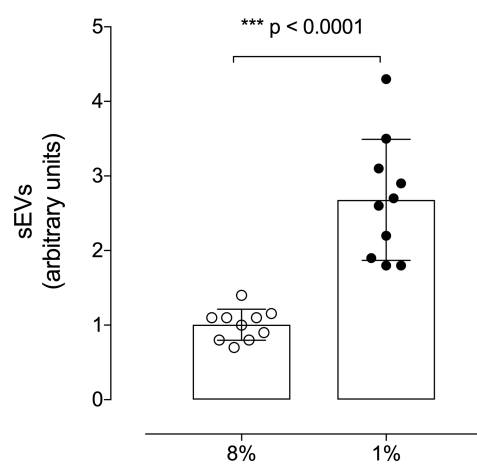
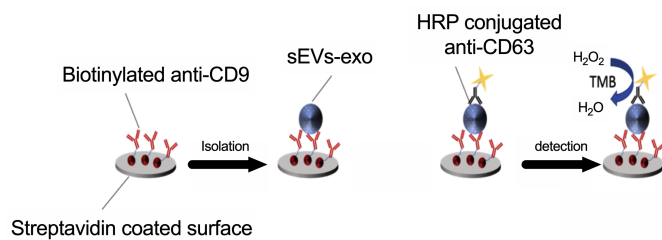
793

794 **Figure 6. Mean heart rate in pregnant rats treated with 1% and 8% hypoxic**
795 **sEVs.** Mean heart rates were continuously monitored *via* telemetry catheters in the
796 femoral artery from gestational day (GD) 14 until GD 21. Mean heart rates are
797 presented in 12-h intervals showing circadian variation; nighttime periods are

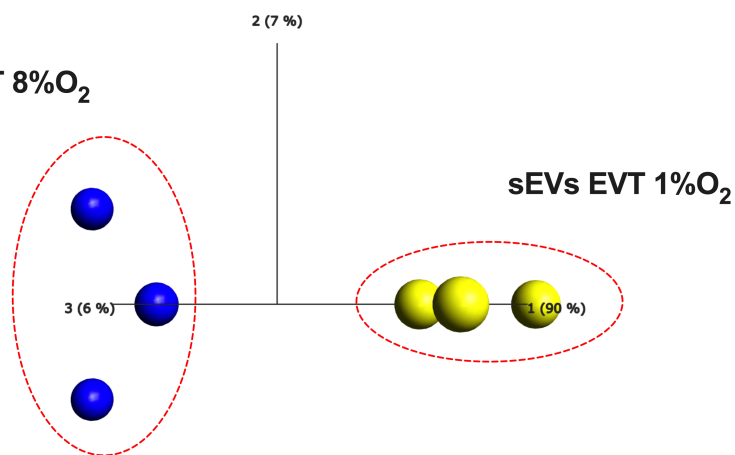
798 shaded. Data points represent the mean \pm SEM of measurements in 6 rats in each
799 group.



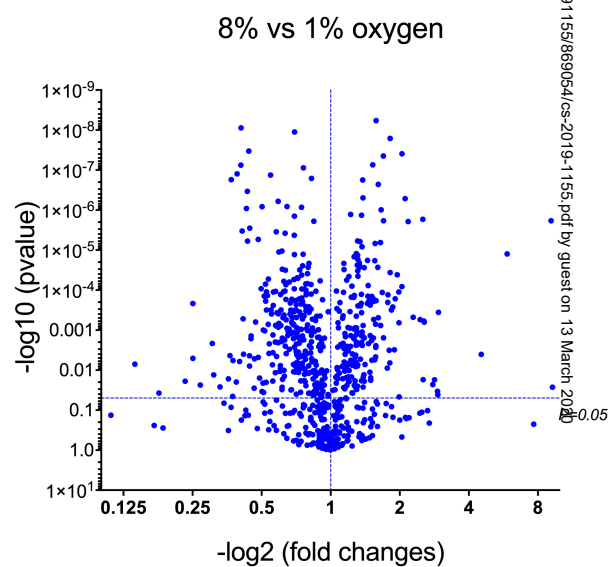
A

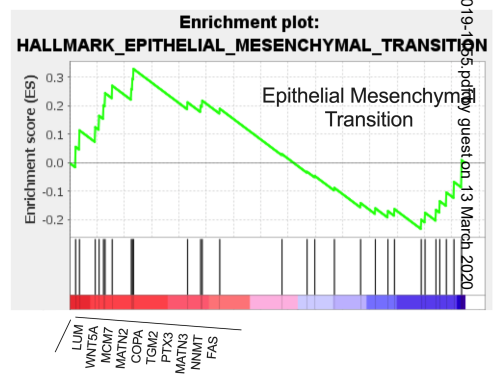
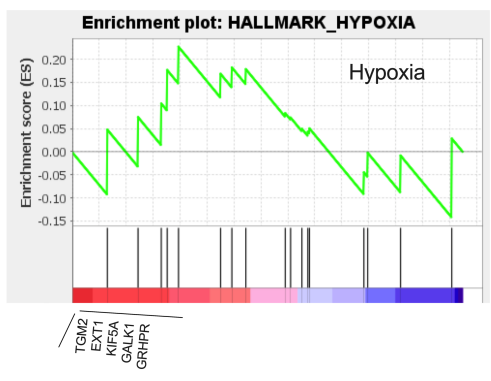
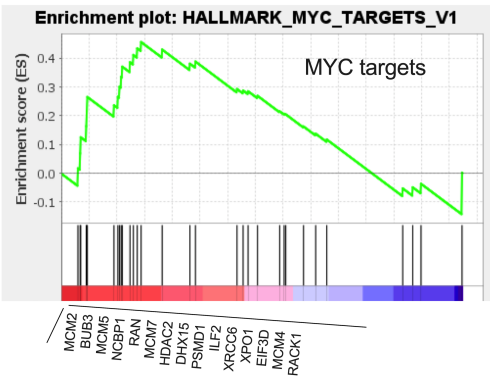
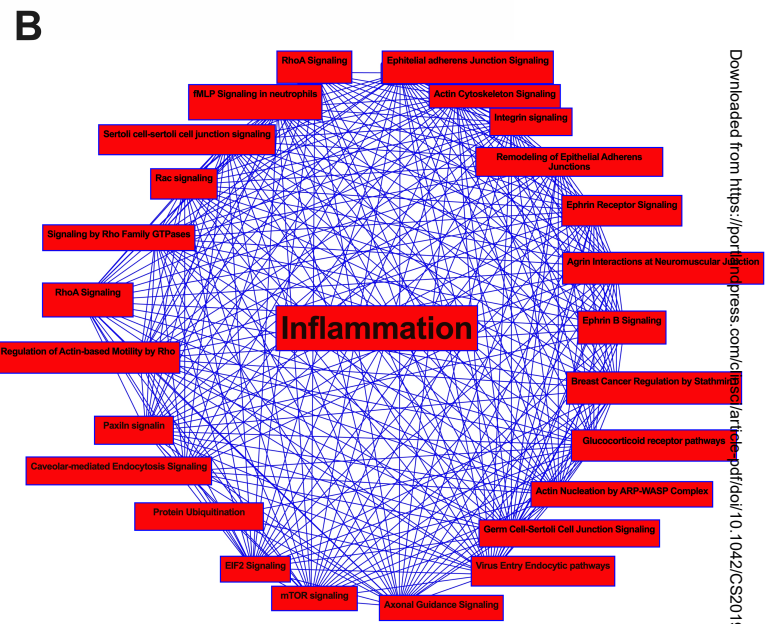
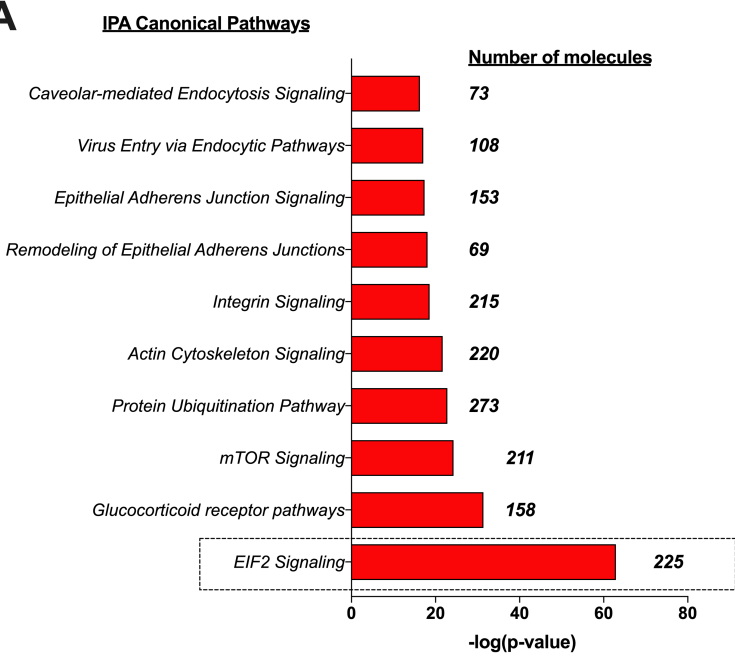


B

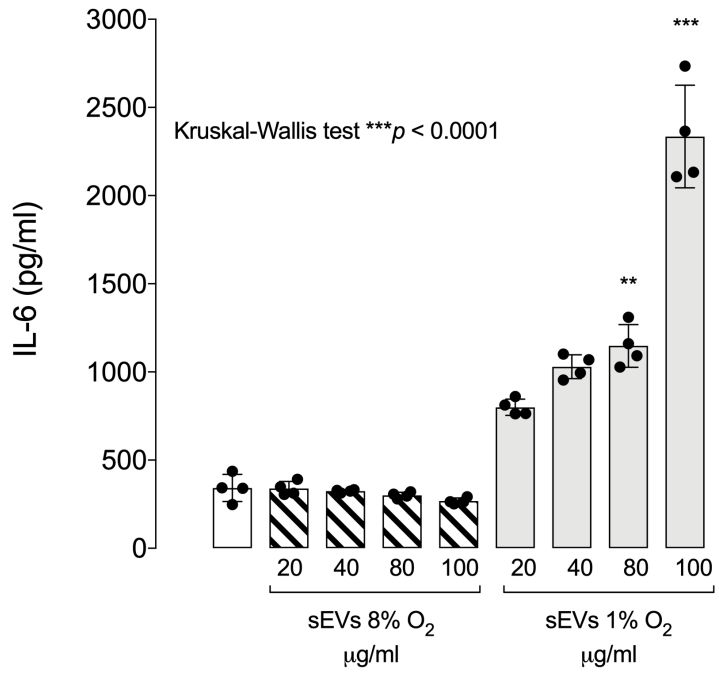


C

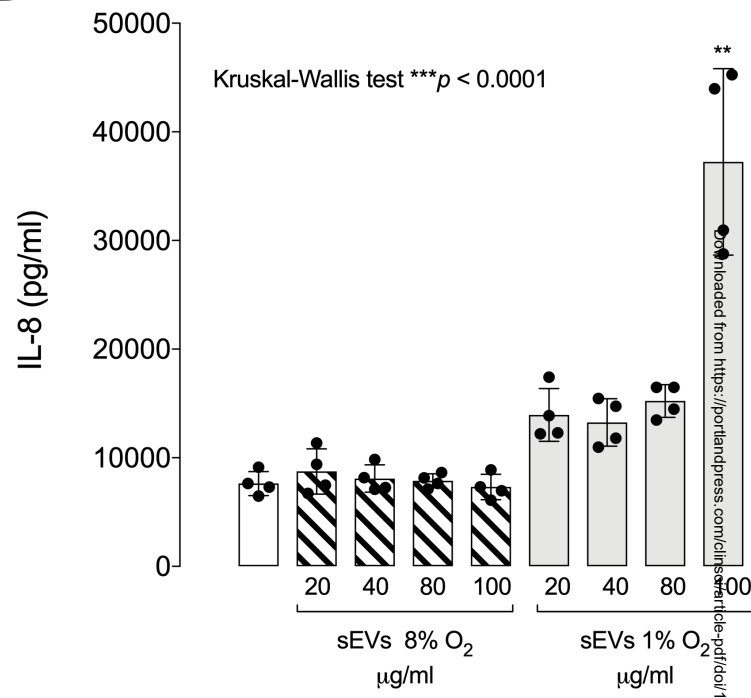




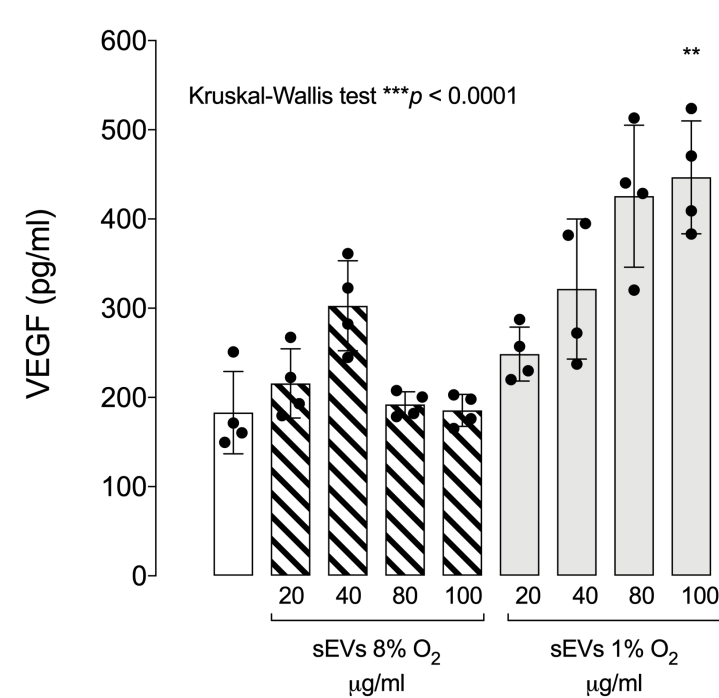
A



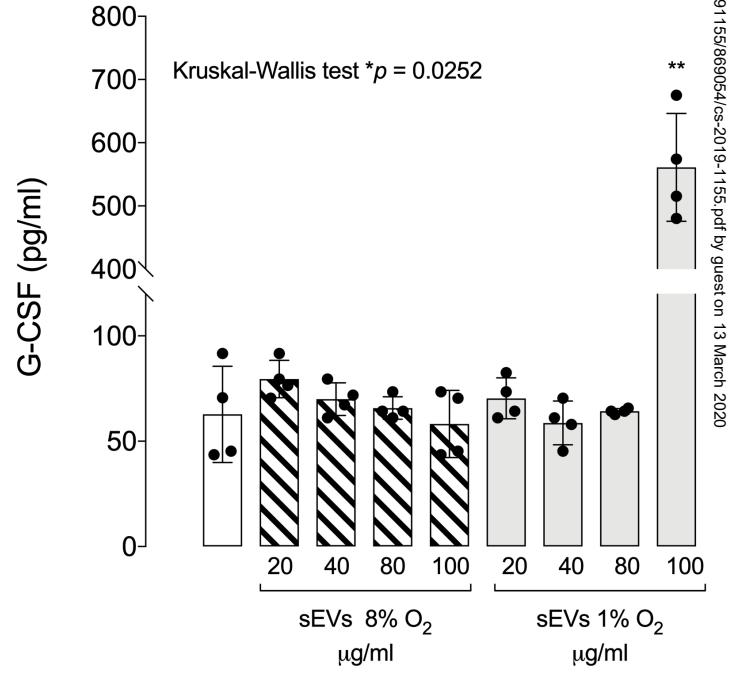
B



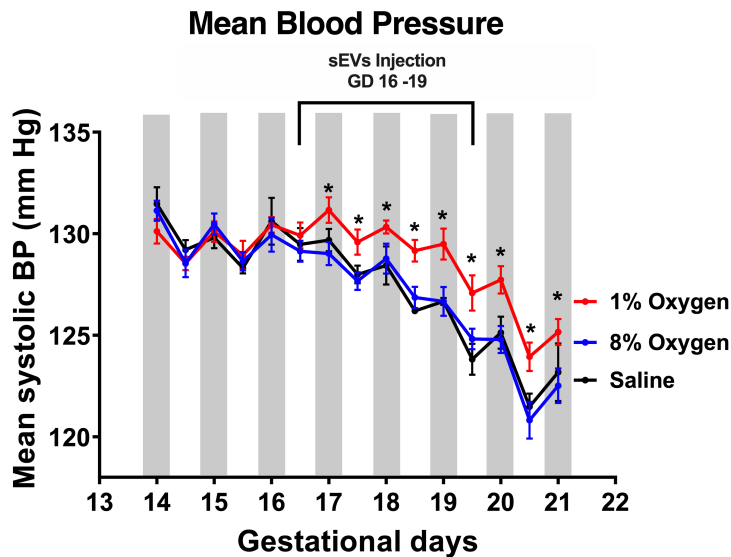
C



D

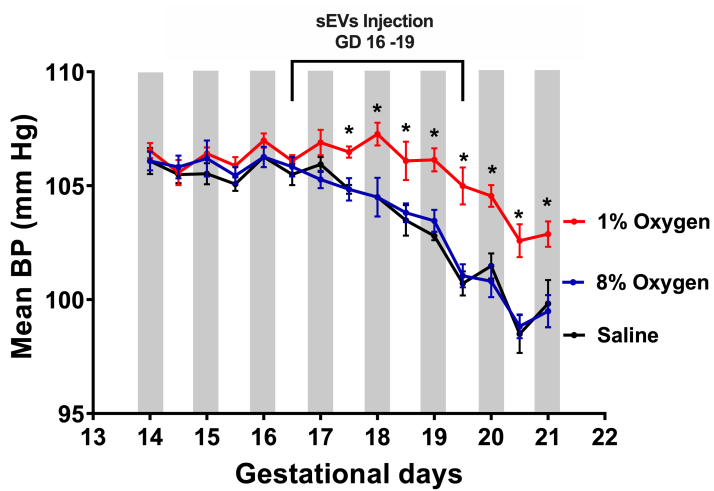


A

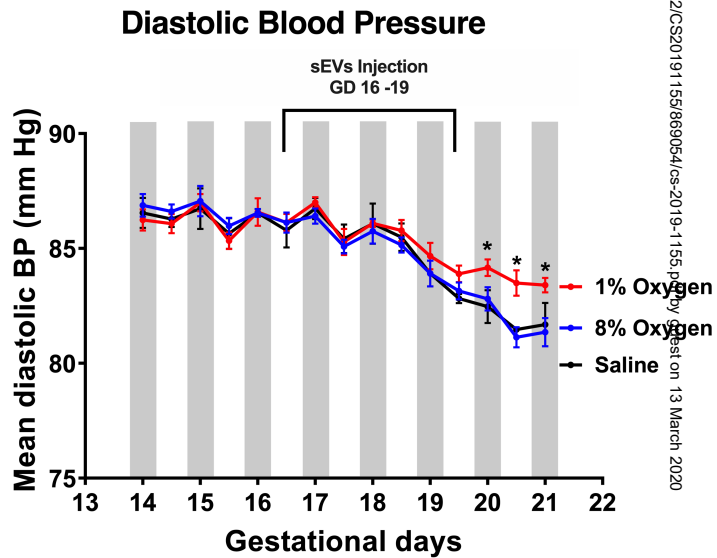


B

Systolic Blood Pressure



C



Mean Heart rate

